COMPUTATIONAL FLUID DYNAMICS SIMULATIONS IN AEROSOL AND NUCLEATION STUDIES

ERIK HERRMANN

Division of Atmospheric Sciences
Department of Physics
Faculty of Science
University of Helsinki
Helsinki, Finland

Academic dissertation

*To be presented, with the permission of the Faculty of Science
of the University of Helsinki, for public criticism in auditorium A129,
A. I. Virtasen aukio 1, on October 8th, 2010, at 12 o'clock noon.*

Helsinki 2010

Acknowledgements

Computational fluid dynamics simulations in aerosol and nucleation studies

Erik Herrmann
University of Helsinki, 2010

Abstract

Nucleation is the first step in the formation of a new phase inside a mother phase. Two main forms of nucleation can be distinguished. In homogeneous nucleation, the new phase is formed in a uniform substance. In heterogeneous nucleation, on the other hand, the new phase emerges on a pre-existing surface (nucleation site). Nucleation is the source of about 30% of all atmospheric aerosol which in turn has noticeable health effects and a significant impact on climate.

Nucleation can be observed in the atmosphere, studied experimentally in the laboratory and is the subject of ongoing theoretical research. This thesis attempts to be a link between experiment and theory. By comparing simulation results to experimental data, the aim is to (i) better understand the experiments and (ii) determine where the theory needs improvement.

Computational fluid dynamics (CFD) tools were used to simulate homogeneous one-component nucleation of n-alcohols in argon and helium as carrier gases, homogeneous nucleation in the water-sulfuric acid-system, and heterogeneous nucleation of water vapor on silver particles. In the nucleation of n-alcohols, vapor depletion, carrier gas effect and carrier gas pressure effect were evaluated, with a special focus on the pressure effect whose dependence on vapor and carrier gas properties could be specified. The investigation of nucleation in the water-sulfuric acid-system included a thorough analysis of the experimental setup, determining flow conditions, vapor losses, and nucleation zone. Experimental nucleation rates were compared to various theoretical approaches. We found that none of the considered theoretical descriptions of nucleation captured the role of water in the process at all relative humidities. Heterogeneous nucleation was studied in the activation of silver particles in a TSI 3785 particle counter which uses water as its working fluid. The role of the contact angle was investigated and the influence of incoming particle concentrations and homogeneous nucleation on counting efficiency determined.

Keywords: homogeneous nucleation, heterogeneous nucleation, classical nucleation theory, computational fluid dynamics

Nomenclature

A	surface area
C	condensation rate
D_p	particle diameter
D	diffusion coefficient
F	force
g	gravitational acceleration
ΔG	free energy of formation
J	nucleation rate
$\vec{J}$	diffusion flux
k	Boltzmann constant
m	mass
μ	chemical potential
$\Delta\mu$	difference of chemical potential between liquid and vapor phase
n	number of molecules
N	number concentration
p	pressure
P	nucleation probability
r	radius (of the cluster)
R	radius (of the seed particle)
RH	relative humidity
ρ	density
S	saturation ratio
S_h	source of heat
σ	surface tension
t	time
T	temperature
θ	contact angle
$\bar{\tau}$	stress tensor
v	molecular volume
$\vec{v}$	velocity
w	molecular weight
ξ	mass fraction of the nucleating species in the gas phase (xi)
Z	Zeldovich non-equilibrium factor

Sub- and superscripts:

act   activated/activation
ave   average
eff   effective
exp   experimental
het   heterogeneous
hom   homogeneous
kin   kinetic
max   maximum
theo   theoretical
g   gas
h   heat
l   liquid
p   particle
v   vapor
*   critical value
A   substance A
B   substance B
1   monomer

Abbreviations:

CFD   computational fluid dynamics
CNC   condensation nuclei counter
CNT   classical nucleation theory
CPC   condensation particle counter (CNC manufactured by TSI
                           Inc., often used as a general name for CNCs)
FPM   Fine Particle Model

Contents

List of publications

This thesis consists of an introductory review followed by five research papers. The articles are reproduced with the permission of the journals concerned.

I   Herrmann, E.; Lihavainen, H.; Hyvärinen, A.-P.; Riipinen, I.; Wilck, M.; Stratmann, F.; Kulmala, M. Nucleation simulations using the fluid dynamics software FLUENT with the fine particle model FPM. J. Phys. Chem. A 2006, 110, 12448-12455.

II Herrmann, E.; Hyvärinen, A.-P.; Brus, D.; Lihavainen, H.; Kulmala, M. Re-evaluation of the Pressure Effect for Nucleation in Laminar Flow Diffusion Chamber Experiments with Fluent and the Fine Particle Model. J. Phys. Chem. A 2009, 113, 1434–1439.

III Herrmann, E.; Brus, D.; Hyvärinen, A.-P.; Stratmann, F.; Wilck, M.; Lihavainen, H.; Kulmala, M. A computational fluid dynamics approach to nucleation in the water-sulfuric acid-system. J. Phys. Chem. A 2010, 114, 8033–8042.

IV Stratmann, F.; Herrmann, E.; Petäjä, T.; Kulmala, M. Modelling Ag-particle activation and growth in a TSI WCPC model 3785. Atmos. Meas. Tech. 2010, 3, 273-281.

V   Kulmala,M.; Mordas, G.; Petäjä, T.; Grönholm, T.; Aalto, P. P.; Vehkamäki, H.; Hienola, A. I.; Herrmann, E.; Sipilä, M.; Riipinen, I.; Manninen, H.; Hämeri, K.; Stratmann, F.; Bilde, M.; Winkler, P. M.; Birmili, W.; Wagner, P. E. The condensation particle counter battery (CPCB): a new tool to investigate the activation properties of nanoparticles, J. Aerosol Sci. 2007, 38, 289-304.

1 Introduction

Aerosols affect life in many different ways. Health effects can be linked to aerosol exposure (e.g. Künzli et al., 2000; Pope et al., 2002); visibility and the overall quality of living suffer from pollution events such as the occasional Russian forest fires (e.g. Lee et al., 2003; Bozier et al., 2007). Aerosols play a role in atmospheric chemistry, affect Earth's radiation budget, cloud formation, weather – in short: the climate (e.g. Twomey, 1974; Twomey, 1984 & 1991; IPCC, 2007). By definition, aerosols are particles suspended in a gas, their sizes ranging from the nanometer scale to tens of micrometers – everything between larger molecules and water droplets just short of turning into rain. The characteristics of an aerosol population (total number concentration, size distribution, chemical composition etc.) depend on the location – Urban or remote rural? Continental or marine? Boundary layer or higher up? - as well as on the season and even the time of the day (e.g. Pöschl, 2005).

Based on their source, aerosols can be divided into two groups: primary aerosols which are directly released into the atmosphere through natural or anthropogenic processes such as wave breaking and burning of fossil fuel or biomass; and secondary aerosols which are formed in the atmosphere: precursor gases become particles by nucleation and condensation (Seinfeld and Pandis, 1997). In the latter case, chemical reactions can play an important role by turning precursor gases into species with low vapor pressure and thus high saturation ratio, i.e. creating favorable conditions for new particle formation.

Nucleation is the first step in a first order phase transition, during nucleation, a new phase is born. The concept of nucleation can be used to describe a wide range of phenomena, and thus the new phase can be gas, liquid, or solid. Besides dew, fog and cloud droplet formation (all gas to liquid), examples for nucleation also include the freezing of a liquid (liquid to solid), the boiling of a liquid, and the spilling over of good German beer after the first over-enthusiastic sip from a newly opened bottle (both liquid to gas). The latter phenomenon has gained considerable attention especially from French researchers, but they, of course, have focused on champagne (e.g. Liger-Belair et al., 2002). The phenomenon also is a "real life" example of the pressure effect, one of the topics of this thesis (section 3.2): bubble formation (i.e. nucleation) starts only after the bottle has been opened (i.e. at lower pressure).

Two types of nucleation can be defined: Homogeneous nucleation is the formation of a new phase in the body of the mother phase, while in heterogeneous nucleation the new phase is formed on a pre-existing surface. Most nucleation events that can be observed in daily life are heterogeneous, simply because there are always surfaces (or impurities) available. One example is the fogging of glasses when entering a warm room on a cold and preferably moist day. Even ice formation at 0°C is heterogeneous: Fahrenheit (1724) found that boiled, air-free water was still liquid after being kept for hours at -9°C, today the supercooling limit has been established at -42°C (Debenedetti and Stanley, 2003).

Besides this division into homogeneous and heterogeneous, nucleation phenomena can

also be classified based on the number of species taking part in the phase transition. There is one-component (unary) nucleation and multi-component nucleation, where the latter one can be more accurately divided into two-component (binary), three-component (ternary) and so on nucleation. In this work, the main focus has been on one- and two-component homogeneous nucleation, but also heterogeneous nucleation has been considered.

In the atmosphere, aerosols have a significant effect on Earth's radiation balance. They reflect incoming light (direct aerosol effect; Twomey, 1974) and they increase the cloud cover and alter the reflective properties of clouds (indirect effect; Twomey, 1991), thus cooling the atmosphere. But they also absorb the incoming radiation's energy, thus heating the surrounding air. This prevents cloud formation (semi-direct effect; Hansen et al., 1997) and thus somewhat counters the above effects. About 30% of the total number of aerosol particles in the atmosphere is a product of nucleation from the gas phase (Spracklen et al., 2006). Nucleation events have been observed all over the globe (Kulmala et al., 2004). Recent geoengineering approaches suggested by Crutzen (2006) and Wingenter et al. (2007) rely on nucleation to produce the particles needed to cool the atmosphere. However, the process of nucleation is not yet fully understood.

Laboratory experiments offer the possibility to study nucleation under well-defined conditions with only known species present. While one-component homogeneous nucleation is an unlikely candidate to explain atmospheric nucleation, it is the simplest form of nucleation to be studied experimentally and theoretically. Experiments in the water-sulfuric acid-system on the other hand might already tell us something about atmospheric nucleation, since sulfuric acid is supposed to play a major role in the process (Seinfeld and Pandis, 1997). However, experiments as such can provide only limited information. Experimental setups often require a model to interpret the measured data, and, generally, models are needed to compare experiment and theoretical prediction and thus be able to improve the theory. To build a new model "from scratch" for every new experiment is a challenging or even impossible task if for example the flow is not laminar or if multiple species are involved in the process.

Despite the potential benefits, computational fluid dynamics (CFD) techniques have so far been used scarcely in aerosol research. In this thesis, the CFD code Fluent together with the Fine Particle Model (FPM) is employed to study aerosol dynamics and especially nucleation. The idea is to "outsource" geometry generation, flow simulation, and mass and heat transfer of our models to CFD and thus be able to focus on the aerosol and nucleation part. Starting with one-component homogeneous nucleation, we will progress towards more complicated processes and setups. Our objectives are to:

- Simulate various forms of nucleation to further our understanding of the nucleation process.

- Verify the carrier gas and the carrier gas pressure effect in the one-component nucleation of *n*-alcohols and improve our understanding of the underlying mechanisms.

- Determine operation conditions in an experiment on nucleation in the sulfuric acid-water-system. What are the flow patterns, where does nucleation take place, what are temperature and sulfuric acid vapor concentration in the nucleation zone - i.e. which conditions and processes lead to the measured particle concentrations?

- Compare measured nucleation rates for water and sulfuric acid with predictions by various nucleation theories. Which theory works best under which conditions? What is thus required of a possible new, better theory?

- Test how well classical heterogeneous nucleation theory describes the operation of a condensation nuclei counter. What is the role of the contact angle? How can the theory be improved?

- Evaluate the feasibility of the CFD approach in aerosol and nucleation modeling. What are the benefits and what the downsides?

2 Nucleation in theory and experiment

The foundations of the classical nucleation theory (CNT) date back the works of Gibbs (1906) who during 1876-1878 developed a thermodynamic theory of curved surfaces. What nowadays is called CNT is the sum of works by Volmer and Weber (1926), Farkas (1927), Becker and Döring (1935), Zeldovich (1942), and Frenkel (1946). The theory was extended by Reiss (1950) to also account for two-component systems.

The central assumption and main shortcoming of the classical nucleation theory is the so-called capillary approximation. This means we use macroscopic properties such as density and surface tension and their bulk liquid values to describe microscopic clusters consisting only of a few molecules for which things such as a well-defined surface do not even exist. Not surprisingly, the predictive powers of CNT are limited, with theoretical and experimental nucleation rate values differing by several orders of magnitude.

Nevertheless, the classical nucleation theory is still widely used in aerosol research since it helps us to understand nucleation at least qualitatively. Despite various efforts to formulate new nucleation theories (see e.g. Laaksonen et al., 1995), the classical theory is one of the few practical theories to be used in atmospheric applications, especially in parameterizations for atmospheric models. More sophisticated approaches to describe nucleation rely on interaction potentials for the nucleating molecules. These potentials can be determined with quantum chemical methods but so far the approach is too computationally expensive to be used in practical applications. Semi-empirical approaches such as the kinetic nucleation theory or cluster activation (see section 2.2.2) describe the general behavior in atmospheric nucleation quite well, but they ignore the role of temperature and relative humidity.

In the following, the classical approach to the types of nucleation relevant to this work will be presented. Starting with homogeneous nucleation for the one-component case (section 2.1), we will then move on to two-component homogeneous nucleation and one of its parameterizations (section 2.2), make an excursion into regions beyond the classical theory (section 2.2.2) and, finally, shortly introduce heterogeneous nucleation (section 2.3).

2.1 One-component homogeneous nucleation

The simplest form of nucleation is homogeneous nucleation of just one species. Let us consider a cluster suspended in supersaturated vapor. The cluster consists of n molecules and, following the capillary approximation, we treat it as spherical liquid droplet with radius r. The vapor temperature is T, the pressure is p. The free energy of formation for the cluster is given by (see e.g. Yue and Hamill, 1979)

$$\Delta G_{\text{hom}} = n\Delta\mu + A\sigma \tag{1}$$

Here, $\Delta\mu$ is the difference of the chemical potentials between the vapor and the liquid phase, $A = 4\pi r^2$ is the surface area of the droplet/cluster, and σ is the surface tension of the droplet against the surrounding gas. With $\Delta\mu = -kT \cdot \ln S$, v_l as the volume of one molecule in the liquid, and thus $n = 4\pi \cdot r^3/(3v_l)$, equation 1 becomes (Seinfeld and Pandis, 1997)

$$\Delta G_{\text{hom}} = 4\pi\sigma \cdot r^2 - \frac{4\pi}{3} \frac{kT \ln S}{v_l} r^3 \tag{2}$$

The free energy change as described by equation 2 contains two terms, typically referred to as surface term (left) and volume term (right). The surface term is always positive which means a free energy increase caused by the formation of the cluster surface. In the case of $S > 1$, the volume term is negative, meaning a free energy decrease which is a result of the change of the chemical potential when going from the supersaturated vapor to the liquid phase. Figure 1 shows how these two energies compete.
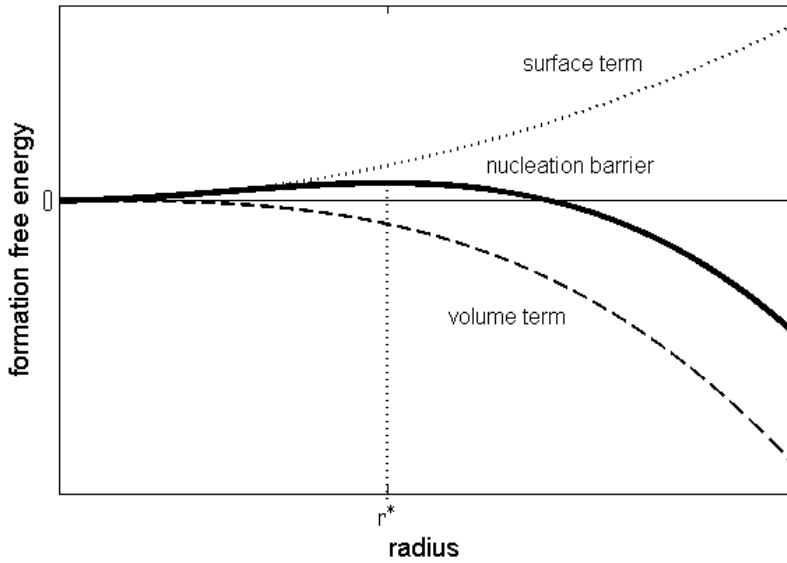
Figure 1. Surface term, volume term, and their sum as a function of cluster radius. The radius of the critical cluster is marked with r^*.

As to be expected from a competition between r^2 and $-r^3$, ΔG_{hom} has a maximum. Before this maximum, molecules energetically prefer to be in the vapor, i.e. evaporate; the cluster is not stable. After the maximum, further growth of the droplet will decrease the free energy of formation; i.e. growth will be energetically favorable and thus continue.

The cluster with the maximum ΔG_{hom} is therefore called the critical cluster; its diameter being the critical diameter. The critical free energy of formation, often referred to as the height of the nucleation barrier, is (Seinfeld and Pandis, 1997):

$$\Delta G_{\text{hom}}^* = \frac{4\pi}{3} r^{*2} \sigma \tag{3}$$

Based on the previous, we can now roughly define a nucleation rate, i.e. the number of clusters growing to sizes larger than the critical size. To do so, we need to know only how many critical clusters there are and a kinetic prefactor that determines how many of them will grow. The concentration of critical clusters can be derived from the equilibrium cluster concentration which simply is the Boltzmann distribution (Seinfeld and Pandis, 1997)

$$N_n = N_1 \exp\left(-\frac{\Delta G_n}{kT}\right) \tag{4}$$

where N_1 is the concentration of monomers, i.e. the vapor concentration. For homogeneous nucleation, the kinetic prefactor is nothing but the average condensation rate C_{ave}. Additionally, the nucleation rate needs to be completed by the Zeldovich non-equilibrium factor Z to account for the difference between the equilibrium cluster concentration and the pseudo-steady state cluster concentration and the possibility that clusters larger than the critical size can still break up to sub-critical sizes. The nucleation rate J thus is (Stauffer, 1976)

$$J = C_{\text{ave}} Z N_1 \exp\left(-\frac{\Delta G^*}{kT}\right). \tag{5}$$

Over the decades, the classical nucleation theory has received much criticism, some of which has lead to widely accepted modifications. The most important of these is the self-consistent correction to rectify the theory's non-zero prediction of the free energy of formation of a monomer. Girshick and Chiu (1990) and Girshick (1991) have simply removed one molecule and its surface contribution from the free energy of formation (equation 2) to solve this problem.

Another target for various improvement attempts has been the classical drop model central to the CNT. Lothe and Pound (1962), for example, calculated a correction factor from the Boltzmann distribution to account for translational and rotational degrees of freedom of the cluster that contributed to the free energy. The semiphenomenological drop model by Dillmann and Meier (1989 & 1991) multiplied the surface term (Eq. 2) with a factor to account for the difference between a microscopic cluster and a macroscopic droplet.

For some systems, improvements such as the ones described above yield good results but the general performance of the classical nucleation theory has not improved. This

explains why the classical nucleation theory in its original form is still widely used.

2.2 Two-component homogeneous nucleation

As seen above, one-component homogeneous nucleation occurs only if the vapor is supersaturated with respect to the nucleating vapor. With more than one species present, nucleation is also possible if none of the species is supersaturated with respect to the pure substance. It is sufficient that the vapors in the mixture are supersaturated with respect to their solution. To put it simply, the presence of a second (or more) species changes the sign of the volume term in equations 1 and 2 and thus enables nucleation.

As in the case of one-component nucleation, also for two-component nucleation the rate of new particle formation can be expressed as

$$J = K \exp\left(-\frac{\Delta G^*}{kT} \right) \qquad\qquad (6)$$

where ΔG^* is, as before, the free energy of formation of the critical cluster. While in the one-component case ΔG depends on the total number of molecules in the cluster, ΔG now is a function of n_A and n_B, the numbers of molecules of both species. The two-dimensional ΔG from figure 1 thus turns into the three-dimensional surface $\Delta G(n_A, n_B)$. Reiss (1950) showed that this surface has a saddle point which is the minimum height of the nucleation barrier. The detailed formulas for two-component nucleation are omitted here since they are not central to this work.

The calculation of a two-component nucleation rate involves solving a non-linear equation for the critical cluster composition and is thus computationally slow. To save computing time, various parameterizations of two-component nucleation based on classical theory have been derived. In our work, we have used the parameterization for the nucleation of water and sulfuric acid by Vehkamäki et al. (2002) which decreases computing time by a factor of 1/500. It is valid between 230.15K and 305.15K, relative humidities from 0.01% to 100% and H_2SO_4 concentrations between 10^4 and $10^{11} cm^{-3}$. The parameterization works particularly well for $RH > 30\%$ at room temperature when predicted nucleation rates match experimental ones within experimental error.

2.2.2 Sulfuric acid nucleation: Beyond classical theory

Sulfuric acid likely plays a central role in atmospheric nucleation (Seinfeld and Pandis, 1997). For example Clarke et al. (1998) found that the two-component nucleation of water and sulfuric acid may explain particle formation in the stratosphere and in the upper troposphere. However, classical two-component nucleation cannot explain nucleation events observed in the lower troposphere. Theoretical approaches to solve the problem often include additional substances. A long-time favorite was three-component

(ternary) nucleation, involving besides water and sulfuric acid also ammonia (Korhonen et al., 1999). More recently, organics have been suggested to play a role in the process (e.g. O'Dowd et al., 2002; Bonn and Moortgat, 2003). Finally, Sipilä et al. (2010) found in their experiments at ambient sulfuric acid concentrations that water and sulfuric acid alone could produce similar nucleation rates as observed in the atmosphere - without a third species involved. The mechanism behind these events, however, is unclear, and classical two-component nucleation is not necessarily the best answer. That's why we have compared the classical approach to two alternative theories which have been suggested to play a role in atmospheric nucleation (**Paper III**). Already in 1980, McMurry suggested a collision-controlled or kinetic mechanism where the particle production rate is

$$J_{kin} = K \cdot \left[H_2SO_4 \right]^2 .$$
(7)

Here, K is a kinetic coefficient and $[H_2SO_4]$ the sulfuric acid vapor concentration. Recent atmospheric measurements locate K between 10^{-14} and $10^{-11} cm^3 s^{-1}$ (Sihto et al., 2006; Riipinen et al., 2007; Kuang et al., 2008). A rather new approach to explain nucleation is the activation of pre-existing clusters proposed by Kulmala et al. (2006). In this cluster activation theory, the nucleation rate can be expressed as

$$J_{act} = A \cdot \left[H_2SO_4 \right]$$
(8)

where A is the activation coefficient. For atmospheric data, A has been found to range from 10^{-7} to $10^{-5} s^{-1}$ (Sihto et al., 2006; Riipinen et al., 2007).

2.3 Heterogeneous nucleation

In heterogeneous nucleation, the existence of a surface on which droplets will be formed fundamentally changes the geometry of the process. In the following, we will assume this surface to consist of spherical seed particles. In homogeneous nucleation, forming droplets are considered spheres. In the heterogeneous case, the cluster is part of a sphere which is attached to the surface of an insoluble seed particle. The angle between cluster and seed particle surfaces is called the contact angle (see figure 2). It depends on the interfacial tensions of the three phases involved: the seed particle, the cluster, and the surrounding gas. The radius of the critical cluster is the same as in the homogeneous case, since it is function only of vapor saturation. However, the critical cluster contains fewer molecules and has a smaller gas-liquid surface area which will affect both the surface and the volume term in equations 1 and 2. Geometrical considerations for the heterogeneous formation energy yield (Lazaridis et al., 1992)

$$\Delta G_{het}^* = \Delta G_{hom}^* \cdot f(m, X)$$
(9)

where the geometric factor is

$$f(m,X) = 1 + \left(\frac{1-mX}{g}\right)^3 + X^3\left(2 - 3\left(\frac{X-m}{g}\right) + \left(\frac{X-m}{g}\right)^3\right) + 3mX^2\left(\frac{X-m}{g} - 1\right) \quad (10)$$

with

$$g = \sqrt{1 + X^2 - 2mX} \ . \tag{11}$$

The geometric factor depends on the ratio of dry particle radius and critical cluster size through $X = R_{dry}/r^*$ and on the macroscopic contact angle θ through $m = \cos\theta$. For a completely unwettable surface, $\theta = 180°$ and accordingly $f = 1$, we observe homogeneous nucleation. In all other cases $f < 1$ which means that pre-existing particles lower the nucleation barrier.
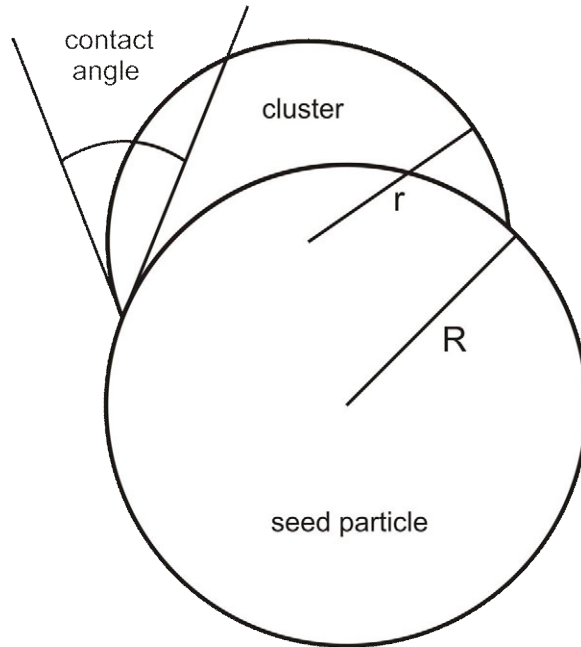
Figure 2. A schematic view of heterogeneous nucleation.

While a nucleation rate for heterogeneous nucleation can be formulated in a very similar manner to the homogeneous case, this heterogeneous nucleation rate is difficult or even impossible to measure. What can be observed experimentally, however, is the proportion of particles that is activated for nucleation in a certain time t. This number is called nucleation probability P (Lazaridis et al., 1992):

$$P = 1 - \exp(-J_{\text{het}} \cdot t) \tag{12}$$

where J_{het} is the nucleation rate per seed particle and unit time. Particles are often assumed to be activated when $P \geq 0.5$. This is called the onset of nucleation.

2.4 Experimental nucleation studies

To study nucleation experimentally, one has to create supersaturation high enough to cross the nucleation barrier. Supersaturation is often achieved by exploiting the fact that heat and vapor diffuse at different rates. Let's for example examine the case where heat diffuses faster than vapor: We have a vapor at temperature T suspended in an inert carrier gas. A slow cooling of the system would merely result in the (excess) vapor condensing on the walls of our setup. If we, however, cool the mixture fast enough, the vapor concentration cannot react to the change as quickly as the temperature. We thus have a cool mixture with "too much" vapor in it, i.e. supersaturation.

One of the first devices to achieve supersaturation was the expansion cloud chamber by Wilson (1897 & 1900), variations of which are still used today (e.g. Strey et al., 1994). In an expansion cloud chamber, supersaturation is achieved by rapid expansion which results in fast adiabatic cooling. Technically, a fast expansion can be realized by moving a piston or opening a valve which connects the initial volume to a low pressure section.

In a laminar flow diffusion chamber (LFDC), a carrier gas is saturated with vapor and then cooled down (or, depending on the vapor, heated up). This results in supersaturation. The LFDC has been used in various nucleation experiments since Anisimov et al. (1978) introduced the method (e.g. Hämeri et al., 1996).

Another common setup to study nucleation is the static diffusion chamber (also called thermal diffusion chamber) (e.g. Katz, 1970; Smolik and Zdimal, 1993) which achieves supersaturation with a different approach. In this chamber, a temperature difference between two plates results in almost linear temperature and vapor pressure profiles between those plates. Since the equilibrium vapor pressure depends exponentially on temperature, this leads to supersaturated conditions near the colder plate.

All the methods described above have been used to study one-component as well as two-component nucleation. Which approach to choose depends on various factors, among them the properties of the nucleating vapor and the desired nucleation rate. In two-component nucleation studies, most recent experiments rely on flow-based techniques (e.g. Ball et al., 1999; Berndt et al., 2006; Young et al., 2008; Sipilä et al., 2010) which are in principle similar to the LFDC described above, if not always necessarily laminar (Brus et al., 2010; **Paper III**).

While homogeneous nucleation experiments are conducted to better understand the nucleation process, heterogeneous nucleation has very practical relevance in aerosol

research. Condensation nuclei counters (CNC) rely on heterogeneous nucleation to activate and subsequently grow small particles to size ranges where they can be optically counted. In principle, a CNC works like a laminar flow diffusion chamber, only with particles added. Naturally, the supersaturation in a CNC has to be set low enough to prevent homogeneous nucleation. Typical working fluids (i.e. the nucleating/condensing vapor) are alcohols and water, but attempts to push the detection limit to smaller and smaller particle sizes have also resulted in the use of more "exotic" substances such as diethylene glycol, for example.

In this work, the focus is on flow-based designs whose basic idea is presented in figure 3. These designs basically consist of two parts. In the "conditioner", the flow is set to a certain temperature and the vapor content is adjusted in such a way that the saturation ratio is 1 or slightly below. In the nucleation or growth tube, the wall temperature differs from the conditioner: Depending on the nucleating vapor, it is higher or lower and the wall works as a vapor source or a vapor sink. In the nucleation or growth tube, the saturation ratio grows over 1, and if the conditions are favorable, nucleation can be observed.
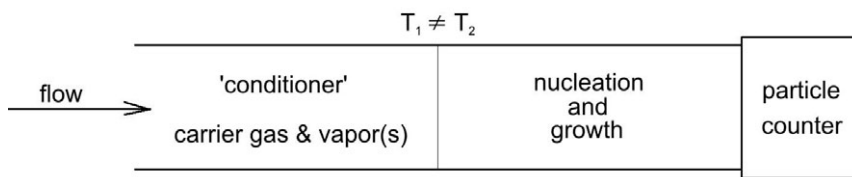
Figure 3. The fundamental design of flow-based nucleation experiments

A major shortcoming of flow tube setups as the one outlined in figure 3 is the fact that they usually do not allow a direct look at the nucleation event and the conditions under which it occurs. Many experimental setups are so small that it would be simply impossible to measure temperature, vapor and particle concentrations inside the tube. And even if the setup is large enough to measure inside the tube, particle number concentration measurements in the nucleation zone are extremely unreliable since newly formed particles are often smaller than the lower detection limits of available particle counters. Thus, while waiting for new experimental methods (e.g. optical detection in the nucleation zone), the only way to gain insight into the nucleation process is to model the experiment and compare the behavior of the model to reliable experimental data.

3 Simulations

3.1 Tools: Computational Fluid Dynamics

Computational fluid dynamics (CFD) is a computer-based tool to simulate the behavior of systems involving fluid flow, heat transfer, mass transfer, and other related physical and chemical processes. The bases of most CFD problems are the Navier-Stokes equations which can be simplified and linearized to yield equations that can be solved numerically. First attempts in the field date back to the 1930s, but the development of the tools used today gained momentum only in the late 1960s when computing resources became available. Since then, progress in CFD has been closely connected to advances in computing power.

The most common solution method used in CFD codes is the finite volume technique. After identifying the region of interest of a given problem (see sections 3.2 – 3.4 for examples), this region is divided into small sub-regions. These are called control volumes or, more instructively, grid cells. The flow equations (or rather discretized versions of them) are then solved iteratively for each control volume to gain an approximation of the value of each variable in each grid cell and thus a full picture of the flow in the simulation domain (Ansys, 2006).

3.1.1 Fluent

In our simulations, we used the CFD code Fluent (Fluent, 2005) which has as of early 2010 been integrated into the Ansys Workbench. Fluent simulates flow based on the Euler equations (simplified versions of the Navier-Stokes equations) for mass (Eq. 13) and momentum (Eq. 14) conservation.

$$\frac{\partial \rho}{\partial t} + \nabla \cdot (\rho \vec{v}) = S_m \tag{13}$$

$$\frac{\partial}{\partial t}(\rho \vec{v}) + \nabla \cdot (\rho \vec{v} \vec{v}) = -\nabla p + \nabla \cdot \overline{\overline{\tau}} + \rho \vec{g} + \vec{F} \tag{14}$$

Here, S_m is a source term, $\overline{\overline{\tau}}$ is the stress tensor, $\vec{g}$ is the gravitational, and $\vec{F}$ the external body force. ρ, v, and p, as usual, stand for density, velocity, and pressure, respectively. These equations are valid for laminar flow. Fluent offers various models to include turbulence in the simulations but those will not be discussed here. In all applications discussed in this work, Fluent also solves the energy equation:

$$\frac{\partial}{\partial t}(\rho E) + \nabla \cdot (\vec{v}(\rho E + p)) = \nabla \cdot \left(k_{\text{eff}} \nabla T - \sum_j h_j \vec{J}_j + (\overline{\overline{\tau}}_{\text{eff}} \cdot \vec{v}) \right) + S_h \qquad (15)$$

Here, k_{eff} is the effective conductivity, and $\vec{J}_j$ is the diffusion flux of species j. The terms on the right represent energy transfer due to conduction, species diffusion, and viscous dissipation, respectively. S_h includes the heat of chemical reaction and other possible volumetric heat sources that have been defined, for example heat released in the condensational growth of particles. A typical Fluent simulation provides information on pressure, density, velocity, temperature, and mass fractions of the species involved for each grid cell of the simulation domain. Fluent's capabilities can be extended by adding user-defined functions (UDF).

3.1.2. Fine Particle Model

The Fine Particle Model (FPM) (Particle Dynamics, 2005) is a complex UDF that adds a particle dynamics model to Fluent. The model provides the possibility to simulate the formation and evolution of particle populations inside a given simulation domain. The processes that can be studied include nucleation, growth, diffusion, and coagulation. The FPM represents the particle size distribution by a superposition of log-normal size distribution functions (modes). To solve the particle dynamic equations, the FPM uses the moment method. This means that integral moments of the modes (e.g. total number) become additional scalars in Fluent. We used the FPM to simulate one-component and two-component homogeneous nucleation as well as heterogeneous nucleation. Necessary details on the equations applied in each case will be presented in the respective chapters 3.2 to 3.4.

3.2 Homogeneous nucleation of *n*-alcohols

Simulations of one-component homogeneous nucleation in a laminar flow diffusion chamber (**Papers I and II**) were performed based on a setup described by Lihavainen and Viisanen (2001). The original experiments were part of the Joint Experiment on Homogeneous Nucleation which aimed at a quantitative comparison between different nucleation rate experiments (Lihavainen, 2000). Nucleating species were *n*-butanol, *n*-pentanol, and *n*-hexanol, with helium or argon acting as the carrier gas. We compared the CFD approach to an earlier model and studied the effect of carrier gas type and pressure on nucleation. **Papers I and II** are based on experimental work published by Lihavainen and Viisanen (2001), Lihavainen et al. (2001), Hyvärinen et al. (2006), and Hyvärinen et al. (2008).
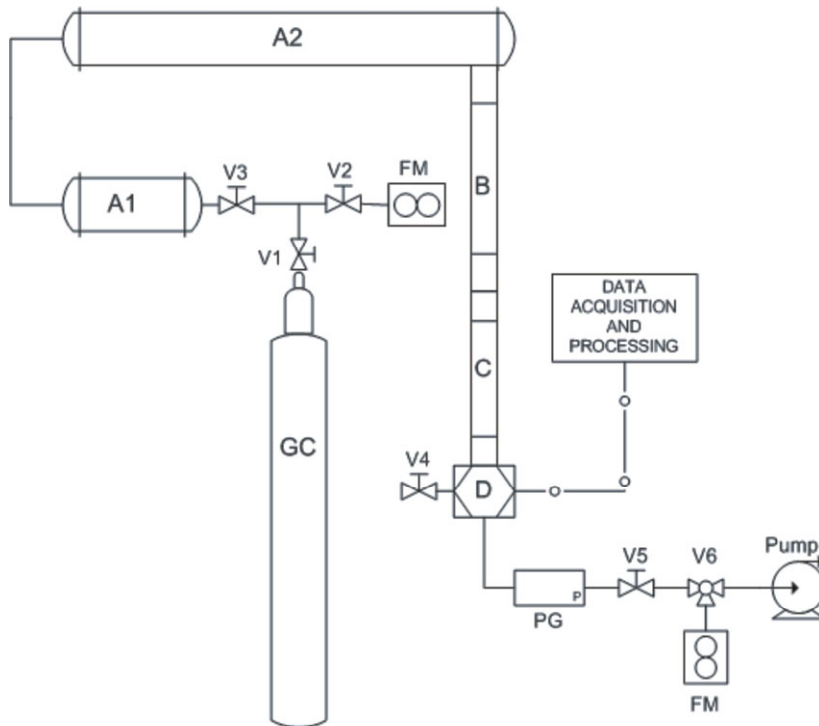
Figure 4. Schematic overview of the laminar flow diffusion chamber (LFDC)

The experimental setup on which the simulations are based is depicted in figure 4. The basic working principle has been described in section 2.4: After being saturated (A1 and A2), the mixture of carrier gas and nucleating vapor enters the preheater (B) whose role it is to ensure well-defined conditions and a laminar flow profile before carrier gas and vapor reach the condenser (C). The walls of the condenser are kept at a lower temperature than the walls of the preheater; the vapor-gas mixture is cooled and becomes supersaturated. Supersaturation depends on the temperature difference ΔT between preheater and condenser; if ΔT is large enough, nucleation will occur. Nucleated particles will grow and can be detected after the flow tube. Preheater and condenser are each 30cm long; their inner diameter is 4mm.

To simulate this setup, only the preheater (B) and condenser (C) were considered, with the saturated vapor-gas mixture coming from the saturator (A) being included as a boundary condition. Since tests have shown the flow to be laminar already a few centimeters into the tube, the simulated preheater is shorter than its experimental counterpart (10cm vs. 30cm). This saves computing time. The condenser, on the other hand, is in the simulation longer than in the experiment (35cm vs. 30cm) to keep simulation boundary effect outside our zone of interest. Exploiting the symmetry of the setup, 2D axisymmetric simulations were performed with grid resolutions of 200000

(**Paper I**) and 250000 (**Paper II**), respectively. The nucleation rate is calculated using the kinetically corrected version of the classical nucleation theory formulation by Becker and Döring (1935)

$$J_{\text{Becker}} = \frac{\left(\rho_g \xi\right)^2}{\rho w} \sqrt{\frac{2\sigma}{\pi w}} \exp\left(-\frac{\Delta G^*}{kT}\right) \cdot \left(\frac{m_p^*}{w}\right)^{2/3} \tag{16}$$

where ξ is the mass fraction of the nucleating species in the gas phase, w is its molecular weight, ρ its liquid density, ρ_g is the (carrier) gas density, and m_p^* is the mass of the critical cluster. Besides nucleation, the Fine Particle Model takes into account particle growth by condensation (including the Kelvin effect), the accompanying heat release, coagulation, particle diffusion, thermophoresis, and gravitational settling.
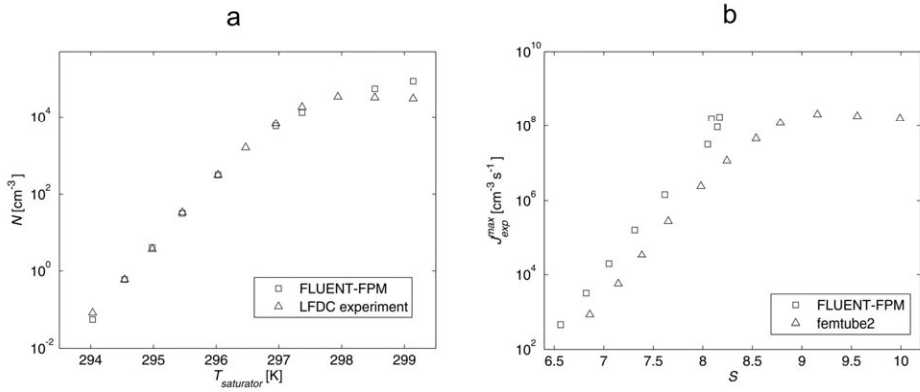

Figure 5. Vapor depletion in the nucleation of n-butanol with helium as the carrier gas. **(a)** Number concentration as a function of saturator temperature (i.e. vapor load) in experiment and simulation. The simulated nucleation rate was corrected using a constant factor of 100000 gained from a comparison of experiment and simulation at low vapor loads. **(b)** An analysis of the same data with two different models, translated into experimental nucleation rate vs. saturation ratio.

In a first step, Fluent-FPM was verified by directly comparing experimental and modeling results. Figure 5a shows how the particle number concentration (simulated and measured) depends on the temperature of the saturator, i.e. the amount of vapor, while all other parameters are kept constant. As expected, particle production grows with saturator temperature – until a certain point. After this point, the available vapor does not turn into higher supersaturations and higher nucleation rates anymore because particles being produced and growing before the hypothetical saturation ratio peak consume so much vapor that this saturation peak gets chopped off. As figure 5a illustrates, Fluent-FPM manages to reproduce this experimentally observed vapor depletion (**Paper I**).

In LFDC experiments it is not possible to directly measure the nucleation rate. Instead,

the maximum experimental nucleation rate J_{exp}^{max} can be determined by combining measurements of particle number concentration at the tube outlet and a model of the experiment. Wagner and Anisimov (1993) have suggested the following formula:

$$J_{exp}^{max} = \frac{J_{theo}^{max}}{N_{theo}} N_{exp} \qquad (17)$$

where N_{exp} is the measured number concentration and J_{theo}^{max} and N_{theo} are the theoretical maximum nucleation rate and the theoretical number concentration, respectively, which both have to be determined using a suitable model. Using this approach, we have compared the Fluent-FPM approach to an earlier model (femtube2) (**Paper I**) and investigated various effects related to the carrier gas (**Papers I and II**).

Figure 5b is the J_{exp}^{max} vs. S interpretation of the data presented in figure 5a. While Fluent-FPM agrees with experimental data according to figure 5a, the agreement with the femtube2 model is rather poor for high saturation ratio values. Figure 5b illustrates a significant difference between the models and its consequences: While Fluent-FPM takes into account the feedback of particle processes on the vapor concentration, femtube2 does not. This means that the models will interpret experimental data at high vapor loads very differently. The figure also shows that Fluent-FPM and femtube2 predict slightly different saturation ratio values for the same setup; the Fluent-FPM value is typically shifted to smaller S. Besides vapor depletion, grid resolution differences are another possible explanation for this. Additionally it has to be pointed out that femtube2 assumes a constant laminar flow profile throughout the tube, ignoring the temperature difference between preheater and condenser and its effects on flow velocity and profile. These differences illustrate some of the benefits of the CFD approach in comparison to "hand-made" models: less assumptions and consequently more accuracy, even though it has to be admitted that these advantages may materialize first and foremost under extreme conditions, like for example vapor depletion at very high S.

After testing the Fluent-FPM model in **Paper I**, we concentrated on the pressure effect in **Paper II**. In nucleation studies, the term "pressure effect" is used to describe the influence of carrier gas total pressure on the nucleation rate observed in the experiment. The nucleation of n-butanol and n-pentanol in helium and of n-pentanol in argon was investigated for pressures ranging from 50kPa to 200kPa and in some cases to 400kPa. In their original analysis of the experimental data, Hyvärinen et al. (2006) had found a significant negative pressure effect for the nucleation of n-butanol in helium. The Fluent-FPM analysis did not, however, confirm these findings, instead the pressure effect for n-butanol was found to be slightly positive, if observable at all. The investigation of this discrepancy revealed a mistake in the femtube2 model and prompted the publication of corrected results (Hyvärinen et al., 2008).
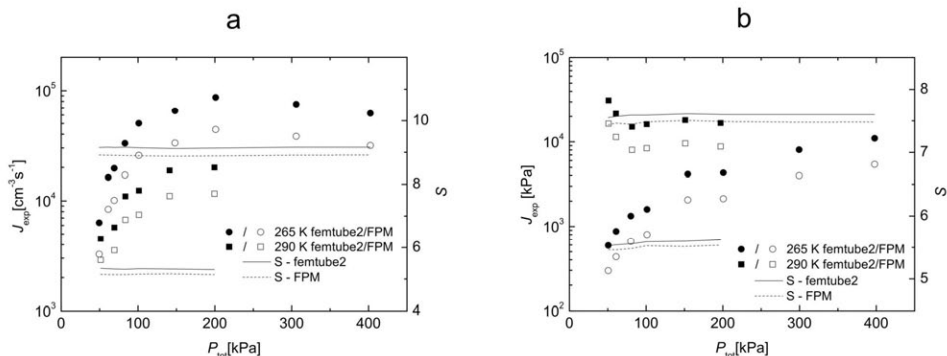
Figure 6. The carrier gas pressure effect in the nucleation of *n*-pentanol in **(a)** helium and **(b)** argon.

Generally, Fluent-FPM results agree well with the corrected femtube2 analysis which in turn is consistent with results from other diffusion-based nucleation experiments (Hyvärinen et al., 2006). Figure 6 shows how the nucleation rate depends on pressure at constant saturation ratio for the nucleation of *n*-pentanol in helium and argon. In the helium case (Fig. 6a), a clear positive pressure effect is observed which is most prominent below 100kPa and levels out beyond 200kPa. For argon (Fig. 6b), the picture is more complicated. At low nucleation temperatures, a positive effect is observed that continues up until 400kPa. At higher nucleation temperatures, a small negative effect can be seen between 50 and 100kPa.

To summarize, negative and positive pressure effects were found, depending on nucleation temperature and carrier gas. This suggests two competing mechanisms at work in the nucleation process, with the negative effect being amplified by a less volatile nucleating species, a heavier carrier gas, and a higher nucleation temperature. According to Wedekind et al. (2008), at low pressures, the effect is a result of the competition between non-isothermal nucleation and the extra work a growing cluster has to do against the pressure of the carrier gas.

In the investigation of one-component homogeneous nucleation, Fluent-FPM showed some advantages when compared to a "hand-made" model. The most important ones are the inclusion of particle feedback on vapor profiles and the more realistic description of the flow, both of which would typically be left out and replaced by assumptions of a well-behaved flow and negligible particle effects. While these simplifications generally work quite well, their validity deteriorates in "extreme" setups, for example at very high saturation ratios. However, Fluent-FPM also exhibited certain shortcomings. One is the lack of control that necessarily accompanies the use of commercial software. This means that simulation strategies depend not only on the nature of the problem at hand but also on the operations that Fluent allows. To the user, Fluent is a black box which is not necessarily ideal in scientific work. Besides these rather general observations, the studies of the pressure effect have highlighted a somewhat unphysical approach to mass conservation. In Fluent, mass is conserved in a way that walls on which a vapor

condenses virtually emit carrier gas to keep the total mass constant. It is possible to work around this unintuitive view on mass conservation but these solutions lead to significantly heavier simulations and are not straight forward.

3.3 Nucleation in the water-sulfuric acid-system
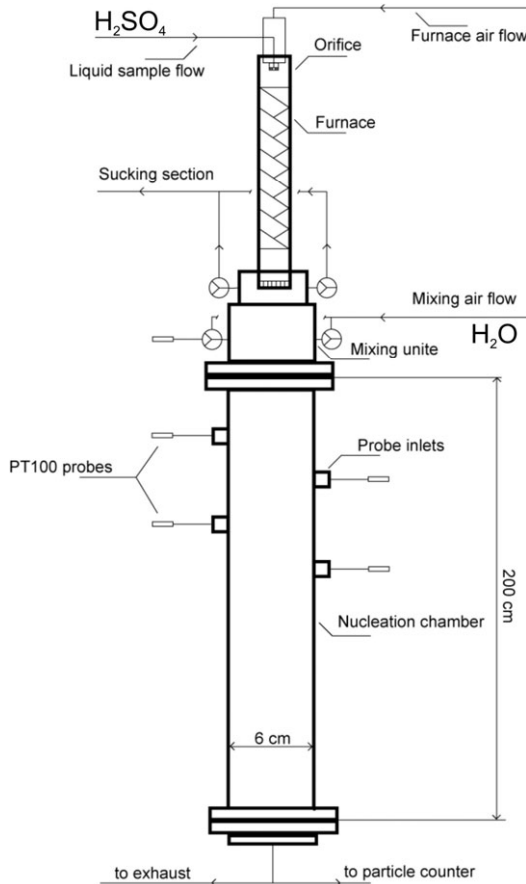
Figure 7. Schematic overview of the flow tube to study nucleation in the sulfuric acid-water-system

Unlike in the one-component case, two-component nucleation experiments are typically not analyzed with the help of detailed numerical models. The reason for this is simply that the level of model complexity rises steeply when the number of involved species grows. Also certain assumptions done for example in the femtube2 model (such as laminar flow) are not necessarily valid in the larger setups used to study two-component nucleation. That is why it is generally not economical to develop models from scratch,

even though the model analysis of the experimental data would deliver valuable insight into the nucleation process as well as into the experimental setup. Since the simulation of multi-species flows is one of its basic applications, CFD can be a solution in this situation. With Fluent taking care of all the vapors and gases involved, only nucleation itself has to considered, and that, too, is possible with reasonable effort within the framework offered by the FPM.

The flow tube (Brus et al., 2010) used to study nucleation in the water-sulfuric acid-system is a close relative of the laminar flow diffusion chamber, if not in its dimensions, then certainly in terms of its working principles. Similar to the LFDC, a mixture of vapors (water and sulfuric acid) and the carrier gas (air) is cooled down, the vapors become supersaturated with respect to their solution, and we observe particle formation. However, the actual setup (figure 7) differs quite substantially from the laminar flow tube described in section 3.2. First of all, the nucleation chamber is 2m long and has an inner diameter of 6cm. For comparison, the respective numbers for the LFDC in section 3.2 are 30cm and 4mm. Also, there is no equivalent to the preheater that would provide well-defined conditions. Sulfuric acid vapor coming from a furnace and humid air are mixed in the turbulent mixing unit, from there the mixture enters the nucleation chamber whose wall is kept at 298.15K. Due to the relative shortness of the mixing unit, the flow profile is not parabolic at the beginning of the nucleation chamber. Additionally, there will be convection which cannot be avoided when downward flow of these dimensions is cooled down. These flow characteristics alone would make the traditional approach with a "hand-made" model rather challenging.

As in the case of the LFDC, also this nucleation chamber is reduced in the simulations (**Paper III**) to a 2D axisymmetric setup. Including the mixing unit with its relatively complicated design and turbulent flow into the calculations would be computationally expensive. Also there would be no possibility to verify the simulation results. Finally, as discussed in **Paper III**, such an exact determination of the inlet boundary conditions is not necessary since the convection zone minimizes the impact of the chosen boundary condition on the simulation results. Thus, only the nucleation chamber itself is considered, assuming well-mixed conditions and – for lack of a better guess – constant flow velocity at the inlet. Furthermore we assume an infinite sulfuric acid sink at the wall and a constant sulfuric acid diffusion coefficient of $0.06cm^2s^{-1}$. Water is expected not to interact with the wall. These assumptions are supported by the currently available experimental data. However, the wall boundary conditions and the actual sulfuric acid diffusion coefficient are heavily entangled issues and as such subject to ongoing research. As pointed out in section 2.2, including the actual formulation of the classical nucleation theory in the model is computationally not feasible. Instead, the parameterization by Vehkamäki et al. (2002) is used which determines the nucleation rate from temperature and vapor concentrations. Nucleation was simulated based on the results published by Brus et al. (2010) for relative humidities of 10%, 30%, and 50% with sulfuric acid vapor concentrations ranging from 10^9 to $3 \cdot 10^{10}cm^{-3}$. With the tube wall at 298.15K, the actual nucleation temperatures are slightly above that value.
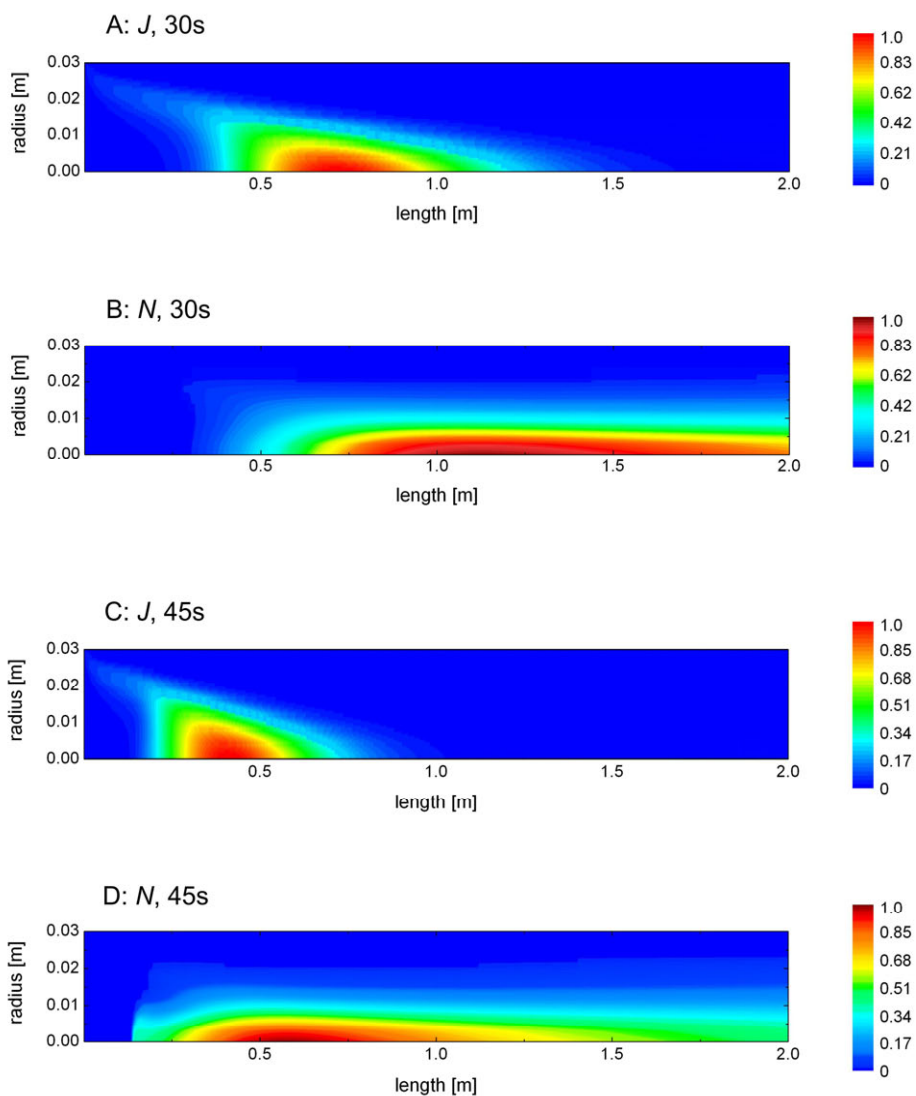
Figure 8. Nucleation zone and its dependence on the average residence time of the gases in the flow tube, viewed from both the J and N perspective. Each figure shows the inside of the tube from the center line (bottom) to the wall (top). The flow enters the tube from the left. J and N are depicted as unit-free relative values.

While experiments of this size in principle offer the opportunity to determine the particle number concentrations also inside the tube (Brus et al., 2010), these measurements are impaired by the lower detection limit of the particle counters involved: The smallest particles cannot always be seen with the instruments available,

even if considerable progress has been made during the last years; Sipilä et al. (2010), for example, report to detect particles as small as 1.5nm. It is even more difficult, if not impossible to measure the actual nucleation rate. With CFD, it is possible to determine at least theoretically where in the tube nucleation occurs. Figure 8 shows the nucleation zone for an example case at 30% relative humidity. It also illustrates how the nucleation zone changes with the flow rate (which is inversely proportional to the residence time) and how it relates to the particle number concentration.

The left column of figure 9 shows a comparison of the experimentally determined nucleation rate to the two-component nucleation rate, the kinetic particle production rate ($K = 2.5 \cdot 10^{-14} cm^3 s^{-1}$, see equation 7), and the cluster activation rate ($A = 10^{-6} s^{-1}$, see equation 8) at 10%, 30%, and 50% relative humidity. We see that the experimental nucleation rate slope is very close to the kinetic theory prediction for $RH = 10\%$ while, at 50% relative humidity, the classical two-component rate best reproduces experimental results. This illustrates the limitations of both theories: While the kinetic approach completely ignores the role of water in the nucleation process, the classical theory seems to overstate the influence of water at low relative humidity and yields good results only at higher RH.

The right column of figure 9 shows a comparison of the measured number concentration to its simulated counterpart which was calculated using the classical two-component nucleation rate. Basically, the curves behave very much like the nucleation rates in the left column, showing good agreement in terms of slope and absolute numbers at 50% relative humidity. However, the right column is significant as it, other than the left column, shows a direct comparison of simulation results to "uninterpreted" experimental data. The right column anchors our simulations in the experimental reality. The right column also allows us to derive nucleation rate correction factors to improve the predictive capabilities of classical theory under similar conditions as in these experiments.

Besides stressing the need for improved nucleation theories, our simulations also highlight the necessity to gain detailed knowledge of the experimental setup. The model in its current state and its results can be considered qualitatively robust (**Paper III**, section 3.6), but a quantitative verification of possible improved nucleation theories would require an in-depth analysis of the main assumptions of the current model. Most importantly, the diffusion coefficient of sulfuric acid in humid air has to be determined more accurately and the wall boundary conditions for sulfuric acid have to be re-considered. Both issues are heavily inter-connected and a possible solution of the problem requires both experimental and computational efforts.
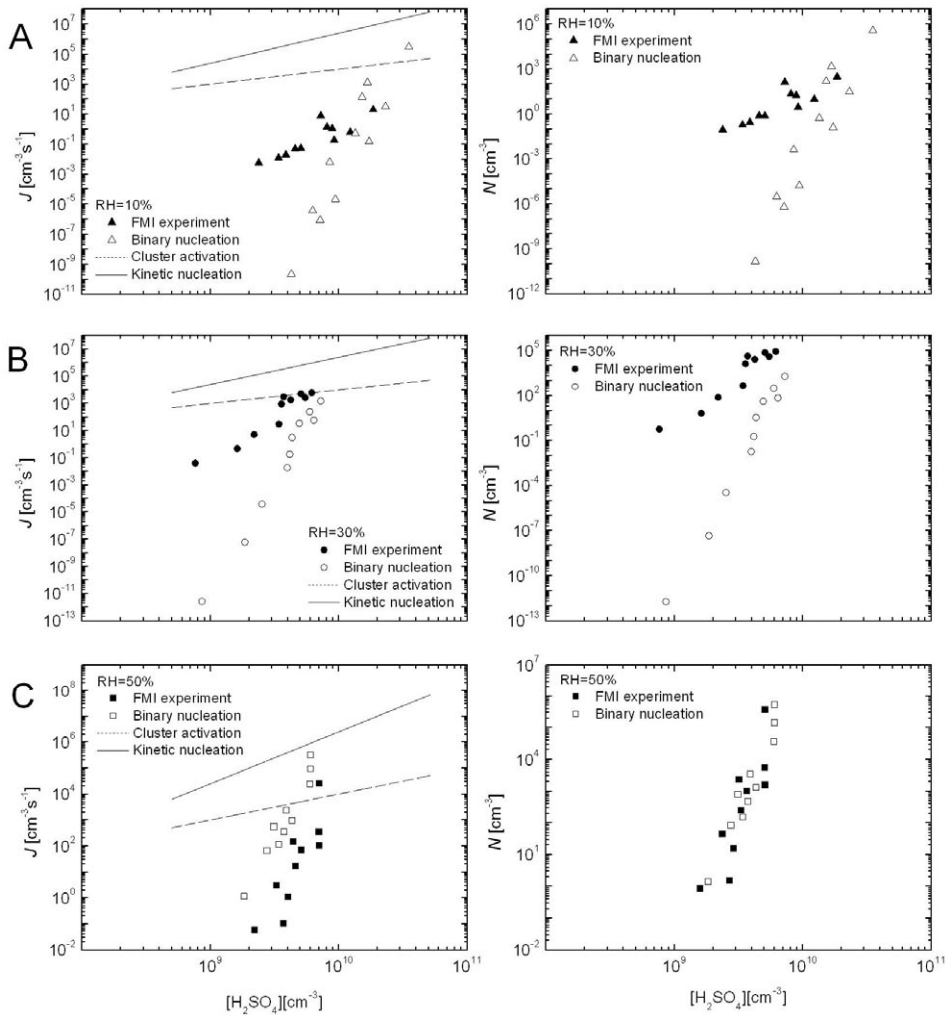
Figure 9. Experimental and various theoretical nucleation rates (left column) and a comparison of experimental and simulated number concentrations (right column).

3.4 Performance of the water-CPC TSI 3785: Heterogeneous nucleation

The TSI 3785 water-CPC has been the subject of two CFD investigations. While in **Paper V** the simulation of the instrument has focused only on water saturation ratio and temperature profiles as part of a larger project, **Paper IV** is a detailed study of the instrument, modeling in detail activation and growth of silver particles to determine the effects of heterogeneous and homogeneous nucleation on the perceived counting efficiency of the device.

Figure 10. Schematic overview of the TSI 3785 water-CPC.

The basic setup of the instrument is simply a tube consisting of two parts (saturator and growth tube) at different temperatures, wetted walls ensuring a relative humidity of 100% at the inner surface. In principle, the TSI 3785 is a laminar flow diffusion

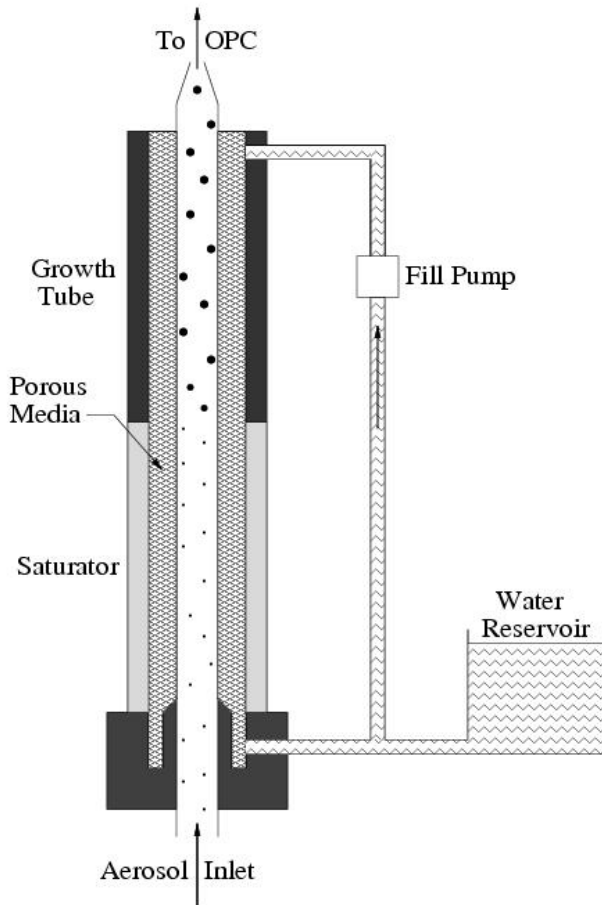chamber, just with particles added: Aerosol enters the tube, the air is then saturated with water in the saturator, and in the growth tube supersaturation leads to activation of the aerosol particles by heterogeneous nucleation and their subsequent growth. Unlike in the case of the LFDC described in section 3.2, the growth tube is kept at a higher temperature than the saturator. This is a consequence of using water as the working fluid; in the case of water, heat and vapor diffusion behave right opposite to the alcohol case. For water, vapor diffuses faster than heat. Figure 11 illustrates this phenomenon and shows the resulting saturation ratio profile as well as the heterogeneous nucleation probability for 6nm seed particles.
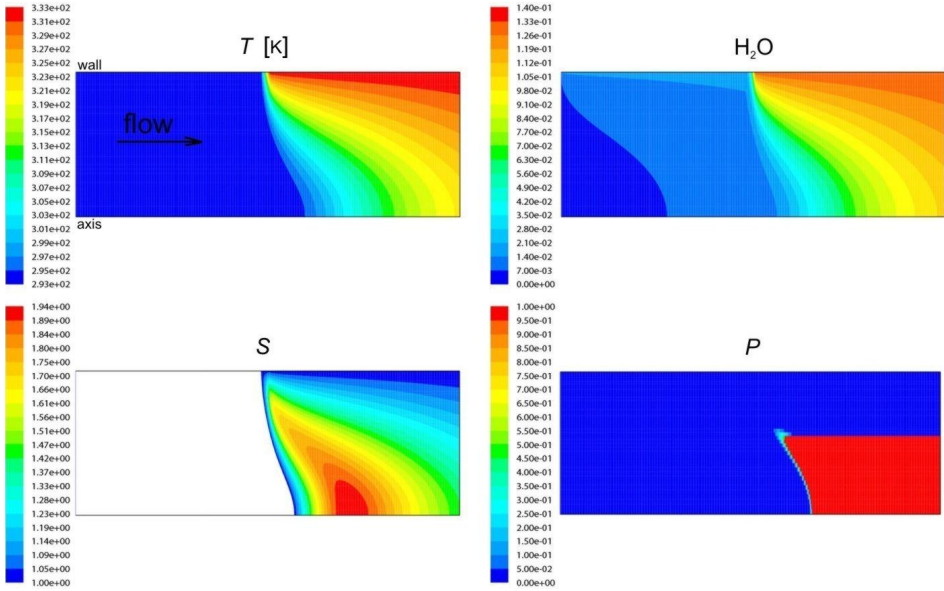
Figure 11. Contours of temperature (upper left panel, T [K]), water vapor mass fraction (upper right panel, H_2O), water vapor saturation ratio (lower left panel, S), and heterogeneous nucleation probability for 6nm seed particles (lower right panel, P) inside the TSI 3785 WCPC with a saturator temperature $T_s = 20°C$ and growth tube temperature $T_{gt} = 60\ °C$.

Heterogeneous nucleation was treated as outlined in section 2.3. As commonly done, particles were assumed to be activated for values of heterogeneous nucleation probability $P \geq 0.5$. Particle growth by condensation was modeled according to Barrett and Clement (1988) to also account for the effect of latent heat release on droplet temperature (see **Paper IV** for details).

The behavior of the instrument was simulated for various contact angles θ, varying temperature differences between saturator and growth tube and different combinations of seed particles. Also the effect of homogeneous nucleation was investigated. For the case of two populations of seed particles of different sizes, model calculations showed

that, at high enough number concentrations, activation and growth of the larger particles will deplete vapor (also see vapor depletion in section 3.2) to such an extent that the detection efficiency for the smaller particles decreases. On the other hand, by increasing the temperature difference between saturator and growth tube too much (over ca. 58°C, see figure 7b in **Paper IV**), the threshold to homogeneous nucleation will be crossed which will result in perceived "counting efficiencies" over 1. These findings are intuitively not surprising, but with the Fluent-FPM model we are able to quantify the effects and determine explicit limits for the conditions under which the TSI 3785 should be operated in terms of total particle load as well as temperature difference which determines the lower detection limit.
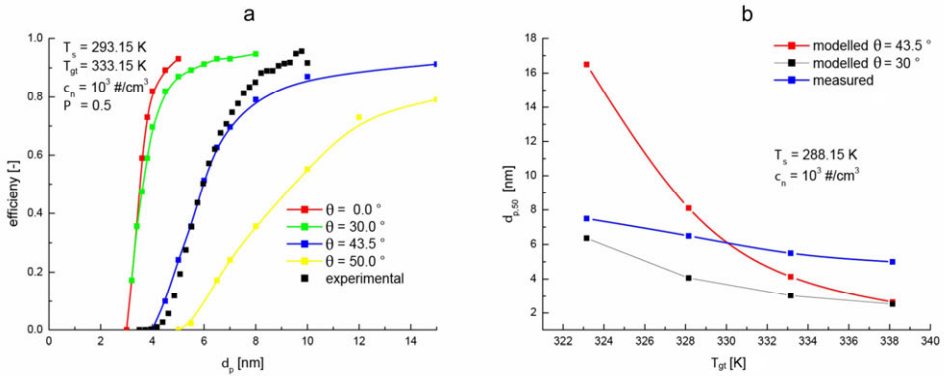
Figure 12. The role of the contact angle in heterogeneous nucleation. **(a)** Counting efficiency as a function of seed particle diameter. **(b)** Cut-off diameter as a function of growth tube temperature.

Concerning the role of the contact angle, simulations of the counting efficiency as a function of seed particle diameter (figure 12a) suggested a contact angle of 43.5° to reproduce experimental results. This value is within the range suggested by Wagner et al. (2005) for silver particles. However, the situation is not quite as simple as figure 12b illustrates. It shows the cut-off diameter as a function of growth tube temperature, simulated for two different contact angles and experimental data. While a contact angle of 43.5° yielded good results in figure 12a, the same angle now produces a picture that differs substantially from experimental findings. At the same time, a contact angle of 30° at least reproduces the general experimental behavior in figure 12b, while being far off the mark in 12a. From these results one has to conclude that classical theory with only the contact angle as a free parameter is not able to coherently reproduce experimental findings. The data presented in figure 12 suggest that, besides the contact angle, also a correction of the kinetic term might be necessary to bring theory and experiment closer together.

4 Review of the papers

This thesis consists of five articles previously published in peer-reviewed journals.

- **Paper I** is dedicated to the one-component homogeneous nucleation of *n*-butanol, *n*-pentanol, and *n*-hexanol in helium and argon. The paper describes the Fluent-FPM model and compares it to experimental results where such a comparison is possible. The CFD approach is then compared to the femtube2 model that has been used earlier. Special focus is on vapor depletion under conditions of extreme vapor load and the carrier gas effect.

- **Paper II** continues the examination of the one-component homogeneous nucleation of *n*-alcohols in helium and argon, now concentrating on the carrier gas pressure effect. An error in the femtube2 model is detected which explains contradictory results that have been found before. We find that the pressure effect depends on the type of carrier gas and the nucleation temperature. The results support the notion that two opposing mechanisms are at work in the nucleation process in such a way that the negative effect is supported by a heavier carrier gas, a higher nucleation temperature, and a less volatile nucleating species.

- **Paper III** expands the field of Fluent-FPM applications towards nucleation in the water-sulfuric acid-system. A nucleating tube is modeled to determine the flow patterns, vapor losses, nucleation zone, and its dependence on flow velocity and relative humidity. Different theoretical nucleation rates are compared to the experimental data. The kinetic nucleation rate shows good agreement at low relative humidity while classical two-component nucleation works better at high *RH*. The results highlight the role of water in the nucleation process which neither the classical nor the kinetic approach seem to predict correctly.

- **Paper IV** is a theoretical investigation of the TSI 3785 particle counter. Fluent-FPM was used to simulate the activation and growth of silver particles inside the instrument. The calculations showed that the presence of larger particles can significantly affect the counting efficiency for smaller particles. We also found that homogeneous nucleation can occur at large temperature differences which will result in a biased total number concentration. The comparison of experiment and simulation revealed that classical nucleation theory with the contact angle as the sole free parameter cannot explain experimental findings consistently.

- **Paper V** presents the condensation particle counter battery (CPCB). The instrument is a combination of four CPCs with different combinations of cut-off size and working liquid (water, *n*-butanol). The instrument is described theoretically, modeled, characterized under laboratory conditions, and tested in the field. The CPCB can be used to study the activation properties of nanoparticles. First results show that growing nucleation mode particles are water-soluble at both 3nm and 11nm.

Author's contribution

I am alone responsible for the summary of this thesis.

In **Papers I, II, and III**, I set up and performed all simulations. I also wrote most of the text for these papers, except for the introduction in **Papers I and II** and the description of the experimental setup in **Paper III**.

In **Paper IV**, I wrote parts of text, most notably the sections describing the instrument, the treatment of heterogeneous nucleation in the simulations, and the transfer of the instrument into a simulation grid. As the corresponding author, I was responsible for all modifications to the manuscript after its initial submission. This process is documented online.

In **Paper V**, I set up and performed the CFD simulations presented and also wrote the respective part of the text.

5 Conclusions

In this thesis, computational fluid dynamics tools are used together with an aerosol dynamics model to study the formation of new particles. To do this, various experimental setups where modeled that investigated a large variety of nucleation phenomena: one- and two-component, homogeneous, and heterogeneous nucleation.

The simplest form of nucleation, one-component homogeneous nucleation, was used as an initial test of the CFD approach. Simulating the nucleation of n-alcohols in helium and argon, the results of a previous model could be confirmed, but details such as the treatment of vapor depletion showed the strength of the new method. The carrier gas and especially the carrier gas pressure effect were investigated in great detail. While not necessarily stressing the advantages of CFD in particular, our work certainly pointed out the advantages of applying a second model to the same problem. The initial data analysis had produced a somewhat confusing picture, and the new model revealed an error in the old one. The new analysis with Fluent-FPM and the corrected femtube2 model yielded a more coherent picture of the carrier gas pressure effect.

Our CFD analysis of nucleation in the water-sulfuric acid-system was the first model of the experimental setup in question. With Fluent-FPM, the flow inside the tube could be simulated and, contrary to the original assumption of a simply laminar flow, we found convection to play a significant role. With CFD, we were able to characterize the nucleation zone and its dependence on relative humidity and flow rate which, at least in such detail, is experimentally impossible. We compared various theoretical nucleation rates to the experimental results and found that the role of water in the formation of new particles is not captured correctly by any of the applied theories. The challenge in devising a working theory of nucleation in the water-sulfuric acid-system lies thus clearly in the understanding of the role of water. Our simulations also point out how to further develop the model in order to obtain more quantitatively reliable results.

Heterogeneous nucleation was studied in the model of the TSI 3785 particle counter. The simulations allow a detailed look into the instrument and a deeper understanding of its working mechanisms. Our results show that the counting efficiency of small particles may decrease if a significant number of larger particles is present. This can be a challenge when for example measuring particle number concentrations in an urban environment where number concentrations are typically very high. The effect as such is not new. We have seen vapor depletion in the nucleation of n-alcohols, and also atmospheric nucleation events are known to be suppressed when large amounts of background aerosol are present to form the so-called condensation sink. But simulations such as ours allow us to quantify the effect and thus correct for it if necessary.

One aspect of this thesis is the evaluation of use of CFD methods in aerosol and nucleation research. The main advantage of Fluent and similar software is certainly the relative ease with which new geometries can be set up and with which flow, heat and mass transfer inside these geometries can be simulated. To create a model of the sulfuric

acid-water tube from scratch, taking into account convection and multi-component diffusion, would be no small challenge. With CFD, all this and the solution algorithms are readily available. A typical problem of commercial software often is its "black box"-character, i.e. limited knowledge as to what the software does exactly. Thus, from a scientist's point of view, more insight into the code and options to manipulate the code would be very welcome. With CFD, one can create very detailed grids and thus perform very detailed simulations, but it needs to be pointed out that these simulations typically take several hours which makes data acquisition a rather time-consuming operation that should be carefully planned. However, a quick CFD look at least at the flow conditions is highly recommended before setting up a new experiment. For example, a Fluent analysis of the large flow tube for sulfuric acid nucleation studies would suggest to turn the experiment upside down in order to avoid dramatic convection effects (see **Paper III**).

To summarize, the main results of this thesis are the following:

- The carrier gas effect and the carrier gas pressure effect in the one-component nucleation of *n*-alcohols were verified. Compared to the initial data analysis, the picture of the pressure effect was clarified. Our analysis suggests that two competing mechanisms affect the nucleation process in such a way that the negative pressure effect is supported by a less volatile nucleating species, a heavier carrier gas, and a higher nucleation temperature.

- Our comparison of experimental data to theoretical predictions of nucleation rates in the water-sulfuric acid-system showed that classical two-component nucleation and kinetic nucleation theory form the boundaries between which the experimentally determined nucleation rate slope will be found, its exact value depending on the relative humidity. At high *RH*, the experimental slope approaches binary theory; at low *RH*, kinetic nucleation is more likely to capture the experimental behavior. The results show that water cannot be ignored in the nucleation process and has to be taken into account in theoretical descriptions of nucleation.

- Considering heterogeneous nucleation in a water-CPC, we found that classical theory with only the contact angle as a free parameter does not explain experimental results in a consistent manner. Our simulations suggest that also a correction to the kinetic term might be necessary to match theory and experiment.

References

Anisimov, M. P.; Kostrovskii, V. G.; Shtein, M. S. Obtaining the supersaturated vapor and aerosol of dibutylphthalate with the mixing of streams of different temperatures by molecular diffusion. *Colloid Journal of the USSR* **1978**, *40*, 90-95.

Anisimov, M. P.; Hämeri, K.; Kulmala,M. Construction and test of laminar flow diffusion chamber: homogeneous nucleation of DBP and *n*-hexanol. *J. Aerosol Sci.* **1994**, *25*, 23-32.

Ansys: *Ansys CFX Release 11.0.* Ansys Inc.: Canonsburg, PA, USA, 2006.

Ball, S. M.; Hanson, D. R.; Eisele, F. L.; McMurry, P. H.: Laboratory studies of particle nucleation: Initial results for H_2SO_4, H_2O, and NH_3 vapors. *J. Geophys. Res.* **1999**, *104*, (D19), 23709-23718.

Barrett, J. C.; Clement, C. F. Growth rates for liquid drops. *J. Aerosol Sci.* **1988**, *19*, 223–242.

Becker, R.; Döring, W. Kinetische Behandlung der Keimbildung in übersättigten Dämpfen. *Ann. Phys. (Leipzig)* **1935**, *24*, 719–752.

Berndt, T.; Böge, O.; Stratmann, F. Formation of atmospheric H_2SO_4/H_2O particles in the absence of organics: A laboratory study. *Geophys. Res. Lett.* **2006**, *33*, L15817.

Bird, R.B.; Stewart, W.E.; Lightfoot, E.N. *Transport Phenomena.* John Wiley & Sons: New York, 1960.

Bonn, B.; Moortgat, G.K. Sesquiterpene ozonolysis: Origin of atmospheric new particle formation from biogenic hydrocarbons. *Geophys. Res. Lett.* **2003**, *30*, 1585.

Bozier, K. E.; Pearson, G. N.; Collier, C. G. Doppler lidar observations of Russian forest fire plumes over Helsinki. *Weather* **2007**, *62*, 203-208.

Brus, D.; Zdimal, V.; Stratmann, F. Homogeneous nucleation rate measurements of 1-propanol in helium: The effect of carrier gas pressure. *J. Chem. Phys.* **2006**, *124*, 43061−430614.

Brus, D.; Hyvärinen, A.-P.; Wedekind, J.; Viisanen, Y.; Kulmala, M.; Zdimal, V.; Smolik, J.; Lihavainen, H. The homogeneous nucleation of 1-pentanol in a laminar flow diffusion chamber: The effect of pressure and kind of carrier gas. *J. Chem. Phys.* **2008**, *128*, 134312.

Brus, D.; Hyvärinen, A.-P.; Viisanen, Y.; Kulmala, M.; Lihavainen, H. Homogeneous nucleation of sulfuric acid and water mixture: experimental setup and first results. *Atmos. Chem. Phys.* **2010**, *10*, 2631-2641.

Clarke, A. D.; Varner, J. L.; Eisele, F.; Mauldin, R. L.; Tanner, D.; Litchy, M. Particle production in the remote marine atmosphere: Cloud outflow and subsidence during ACE 1. *J. Geophys. Res.* **1998**, *103(D13)*, 16397–16409.

Courtney, W. G. Remarks on homogeneous nucleation. *J. Chem. Phys.* **1961**, 35, 2249.

Crutzen, P. J. Albedo enhancement by stratospheric sulfur injections: A contribution to resolve a policy dilemma? *Climatic Change* **2006**, *77*, 211-219.

Debenedetti, P. G.; Stanley, H. E. Supercooled and Glassy Water. *Physics Today* **2003**, *56 (6)*, 40-46.

Dillmann, A.; Meier, G. E. A. Homogeneous nucleation of supersaturated vapours. *Chem. Phys. Lett.* **1989**, *160*, 71-74.

Dillmann, A.; Meier, G. E. A. A refined droplet approach to the problem of homogeneous nucleation from the vapor phase. *J. Chem. Phys.* **1991**, *94*, 3872-3884.

Fahrenheit, D. G. Experimenta & observationes de congelatione aquae in vacuo factae. *Phil. Trans. Roy. Soc.* **1724**, *33*, 78-84.

Farkas, L. Keimbildungsgeschwindigkeit in übersattigten Dämpfen, *Z. Phys. Chem.* **1927**, *125*, 236.

Fluent: *FLUENT 6.2 User's Guide*. Fluent Inc.: Lebanon, NY, USA, 2005.

Frenkel, J. *Kinetic Theory of Liquids*. Oxford University Press: London, 1946.

Gibbs, J. W. *Scientific Papers Vol 1*. Longmans Green: London, 1906.

Girshick, S. L.; Chiu, C.-P.; McMurry, P. H. Time-dependent aerosol models and homogeneous nucleation rates. *Aerosol Sci. Technol.* **1990**, *13*, 465–477.

Girshick, S. L.; Chiu,C.-P. Kinetic nucleation theory: A new expression for the rate of homogeneous nucleation from an ideal supersaturated vapor. *J. Chem. Phys.* **1990**, *93*, 1273−1277.

Girshick, S. Comment on: 'Self-consistency correction to homogeneous nucleation theory'. *J. Chem. Phys.* **1991**, *94*, 826-827.

Hämeri, K.; Kulmala, M.; Krissinel, E.; Kodenyov, G. Homogeneous nucleation in laminar flow diffusion chamber: the operation principles and possibilities for

quantitative rate measurements. *J. Chem. Phys.* **1996**, *105*, 7683–7695.

Hansen, J.; Sato, M.; Ruedy, R. Radiative forcing and climate response. *J. Geophys. Res.* **1997**, *102*, 6831-6864.

Hanson, D. R.; Eisele, F. L. Diffusion of H2SO4 in humidified nitrogen: Hydrated H2SO4. *J. Phys. Chem. A* **2000**, *104*, 1715–1719.

Herrmann, E.; Lihavainen, H.; Hyvärinen, A.-P.; Riipinen, I.; Wilck, M.; Stratmann, F.; Kulmala, M. Nucleation simulations using the fluid dynamics software FLUENT with the fine particle model FPM. *J. Phys. Chem. A* **2006**, *110*, 12448-12455.

Herrmann, E.; Hyvärinen, A.-P.; Brus, D.; Lihavainen, H.; Kulmala, M. Re-evaluation of the Pressure Effect for Nucleation in Laminar Flow Diffusion Chamber Experiments with Fluent and the Fine Particle Model. *J. Phys. Chem. A* **2009**, *113*, 1434–1439.

Herrmann, E.; Brus, D.; Hyvärinen, A.-P.; Stratmann, F.; Wilck, M.; Lihavainen, H.; Kulmala, M. A Computational Fluid Dynamics Approach to Nucleation in the Water-Sulfuric Acid System. . *J. Phys. Chem. A* **2010**, *114*, 8033–8042.

Hussein, T.; Korhonen, H.; Herrmann, E.; Hämeri, K.; Lehtinen, K. E. J.; Kulmala, M. Emission Rates Due to Indoor Activities: Indoor Aerosol Model Development, Evaluation, and Applications. *Aerosol Sci. Tech.* **2005**, *39*, 1111-1127.

Hyvärinen, A.-P.; Lihavainen, H.; Viisanen, Y.; Kulmala, M. Homogeneous nucleation rates of *n*-alcohols in a laminar flow diffusion chamber. *J. Chem. Phys.* **2004**, *120*, 11621−11633.

Hyvärinen, A.-P.; Brus, D.; Zdimal, V.; Smolik, J.; Kulmala, M.; Viisanen, Y.; Lihavainen, H. The carrier gas pressure effect in a laminar flow diffusion chamber, homogeneous nucleation of *n*-butanol in helium. *J. Chem. Phys.* **2006**, *124*, 43041−430411.

Hyvärinen, A.-P.; Brus, D.; Zdimal, V.; Smolik, J.; Kulmala, M.; Viisanen, Y.; Lihavainen, H. Erratum: The carrier gas pressure effect in a laminar flow diffusion chamber, homogeneous nucleation of *n*-butanol in helium [*J. Chem. Phys.* 2006, *124*, 224304]. *J. Chem. Phys.* **2008**, *128*, 109901.

IPCC 2007: Solomon, S.; Qin, D.; Manning, M.; Chen, Z.; Marquis, M.; Averyt, K. B.; Tignor, M.; Miller, H. L. (eds.). *Climate Change 2007: The Physical Science Basis - Contribution of Working Group I to the Fourth Assessment Report of the Intergovernmental Panel on Climate Change.* Cambridge University Press: Cambridge, United Kingdom and New York, NY, USA, 2007.

Johnson, B. T.; Shine, K. P.; Forster, P. M. The semi-direct aerosol effect: Impact of

absorbing aerosols on marine stratocumulus. *Q. J. R. Meteorol. Soc.* **2004**, *130*, 1407–1422.

Katz, J. L. Condensation of a Supersaturated Vapor. I. The Homogeneous Nucleation of the *n*-Alkanes. *J. Chem. Phys.* **1970**, *52*, 4733-4748.

Korhonen, P.; Kulmala, M.; Laaksonen, A.; Viisanen, Y.; McGraw, R.; Seinfeld, J. H. Ternary nucleation of H_2SO_4, NH_3, and H_2O in the atmosphere. *J. Geophys. Res. - Atmospheres* **1999**, *104*, 26349–26353.

Kuang, C.; McMurry, P. H.; McCormick, A. V.; Eisele, F. L. Dependence of nucleation rates on sulfuric acid vapor concentration in diverse atmospheric locations. *J. Geophys. Res.* **2008**, *113*, (D10), D10209.

Kulmala, M.; Vehkamäki, H.; Petäjä, T.; Dal Maso, M.; Lauri, A.; Kerminen, V.-M.; Birmili, W. and McMurry, P.H. Formation and growth rates of ultrafine atmospheric particles: A review of observations. *J. Aerosol Sci.* **2004**, *35*, 143-176.

Kulmala, M.; Lehtinen, K. E. J.; Laaksonen, A. Cluster activation theory as an explanation of the linear dependence between formation rate of 3nm particles and sulphuric acid concentration. *Atmos. Chem. Phys.* **2006**, *6*, 787-793.

Kulmala, M.; Mordas, G.; Petäjä, T.; Grönholm, T.; Aalto, P. P.; Vehkamäki, H.; Hienola, A. I.; Herrmann, E.; Sipilä, M.; Riipinen, I.; Manninen, H.; Hämeri, K.; Stratmann, F.; Bilde, M.; Winkler, P. M.; Birmili, W.; Wagner, P. E. The condensation particle counter battery (CPCB): a new tool to investigate the activation properties of nanoparticles. *J. Aerosol Sci.* **2007**, *38*, 289-304.

Künzli, N.; Kaiser, R.; Medina, S.; Studnicka, M.; Chanel, O.; Filliger, P.; Herry, M.; Horak Jr, F.; Puybonnieux-Texier, V.; Quénel, P.; Schneider, J.; Seethaler, R.; Vergnaud, J.-C.; Sommer, H. Public-health impact of outdoor and traffic-related air pollution: a European assessment. *Lancet* **2000**, *356*, 795-801.

Laaksonen, A.; Talanquer, V.; Oxtoby, D. W. Nucleation: Measurements, theory, and atmospheric applications. *Ann. Rev. Phys. Chem.* **1995**, *46*, 489-524.

Lazaridis, M.; Kulmala, M.; Laaksonen, A. Binary heterogeneous nucleation of a water-sulphuric acid system: The effect of hydrate interaction. *J. Aerosol Sci.* **1991**, *22*, 823-830.

Lazaridis, M.; Kulmala, M.; Gorbunov, B. Heterogeneous Nucleation at a non-uniform surface, *J. Aerosol Sci.* **1992**, *23*, 457-466.

Lee, K. H.; Kim, J. E.; Kim, Y. J.; Kim, J.; von Hoyningen-Huene, W. Impact of the smoke aerosol from Russian forest fires on the atmospheric environment over Korea during May 2003. *Atmos. Environ.* **2005**, *39*, 85-99.

Liger-Belair, G.; Vignes-Adler, M.; Voisin, C.; Robillard, B.; Jeandet, P. Kinetics of Gas Discharging in a Glass of Champagne: The Role of Nucleation Sites. *Langmuir* **2002**, *18*, 1294–1301.

Liger-Belair, G.; Voisin, C.; Jeandet, P. Modeling Nonclassical Heterogeneous Bubble Nucleation from Cellulose Fibers: Application to Bubbling in Carbonated Beverages. *J. Phys. Chem. B* **2005**, *109*, 14573–14580.

Liger-Belair, G.; Parmentier, M.; Jeandet P. Modeling the Kinetics of Bubble Nucleation in Champagne and Carbonated Beverages. *J. Phys. Chem. B* **2006**, *110*, 21145–21151.

Lihavainen, H. A. *Laminar Flow Diffusion Chamber for Homogeneous Nucleation Studies*. Ph.D. Thesis, University of Helsinki, Helsinki, Finland, 2000.

Lihavainen, H.; Viisanen, Y.; Kulmala, M. Homogeneous nucleation of *n*-pentanol in a laminar flow diffusion chamber. *J. Chem. Phys.* **2001**, *114*, 10031−10038.

Lihavainen, H.; Viisanen,Y. A laminar flow diffusion chamber for homogeneous nucleation studies. *J. Phys. Chem. B* **2001**, *105*, 11619−11629.

Lothe, J.; Pound, G. M. Reconsiderations of Nucleation Theory. *J. Chem. Phys.* **1962**, *36*, 2080-2085.

McMurry, P. H. Photochemical aerosol formation from SO_2: A theoretical analysis of smog chamber data. *J. Colloid Interface Sci.* **1980**, *78*, 513-527.

O'Dowd, C.D.; Aalto, P.; Hämeri, K.; Kulmala, M.; Hoffmann, T. Aerosol formation: Atmospheric particles from organic vapours, *Nature* **2002**, *416*, 497-498.

Particle dynamics: *Fine Particle Model (FPM) for FLUENT*. Particle Dynamics GmbH: Leipzig, Germany, 2005.

Pope III, C. A.; Burnett, R. T.; Thun, M. J.; Calle, E. E.; Krewski, D.; Ito, K.; Thurston, G. D. Lung Cancer, Cardiopulmonary Mortality, and Long-term Exposure to Fine Particulate Air Pollution. *JAMA* **2002**, *287*, 1132-1141.

Pöschl, U. Atmospheric Aerosols: Composition, Transformation, Climate and Health Effects. *Angew. Chem. Int. Ed.* **2005**, *44*, 7520 – 7540.

Reiss, H. The Kinetics of Phase Transitions In Binary Systems. *J. Chem. Phys.* **1950**, *18*, 840-848.

Reiss, H.; Margolese, D. I.; Schelling, F. J. Experimental study of nucleation in vapor mixtures of sulphuric acid and water. *J. Colloid Interf. Sci.* **1976**, *56*, 511–526.

Riipinen, I.,; Sihto, S.-L.; Kulmala, M.; Arnold, F.; Dal Maso, M.; Birmili, W.; Saarnio, K.; Teinilä, K.; Kerminen, V.-M.; Laaksonen, A.; Lehtinen K.E.J. Connections between atmospheric sulphuric acid and new particle formation during QUEST III-IV campaigns in Heidelberg and Hyytiälä. *Atmos. Chem. Phys.* **2007**, *7*, 1899-1914.

Seinfeld, J. H.; Pandis, S. N. *Atmospheric Chemistry and Physics: From air pollution to climate change*. Wiley: New York, 1997.

Sihto, S.-L.; Kulmala, M.; Kerminen, V.-M.; Dal Maso, M.; Petäjä, T.; Riipinen, I.; Korhonen, H.; Arnold, F.; Janson, R.; Boy, M.; Laaksonen, A.; Lehtinen, K. E. J. Atmospheric sulfuric acid and aerosol formation: implications from atmospheric measurements for nucleation and early growth mechanisms. *Atmos. Chem. Phys.* **2006**, *6*, 4079–4091.

Sipilä, M.; Berndt, T.; Petäjä, T.; Brus, D.; Vanhanen, J.; Stratmann, F.; Patokoski, J.; Mauldin, R. L.; Hyvärinen, A.-P.; Lihavainen H.; Kulmala, M. The role of sulfuric acid in atmospheric nucleation. *Science* **2010**, *327*, 1243 -1246.

Smolik, J.; Zdimal, V. Condensation of supersaturated vapors. Homogeneous nucleation of bis(2-ethyl-hexyl)sebacate (DEHS*). J. Aerosol Sci.* **1993**, *24*, 589-596.

Spracklen, D. V.; Carslaw, K. S.; Kulmala, M.; Kerminen, V.-M.; Mann, G. W.; Sihto, S.-L. The contribution of boundary layer nucleation events to total particle concentrations on regional and global scales, *Atmos. Chem. Phys.* **2006**, *6*, 5631-5648.

Stauffer, D. Kinetic theory of two-component ('heteromolecular') nucleation and condensation. *J. Aerosol Sci.* **1976**, *7*, 319-333.

Stratmann, F.; Herrmann, E.; Petäjä, T.; Kulmala, M. Modelling Ag-particle activation and growth in a TSI WCPC model 3785. *Atmos. Meas. Tech.* **2010**, *3*, 273-281.

Strey, R.; Wagner, P. E.; Viisanen, Y. The Problem of Measuring Homogeneous Nucleation Rates and the Molecular Contents of Nuclei: Progress in the Form of Nucleation Pulse Measurements. *J. Phys. Chem.* **1994**, *98*, 7748–7758.

Twomey, A. Pollution and the planetary albedo. *Atmos. Environ.* **1974**, *8*, 1251–1256.

Twomey, S.; Piepgrass, M.; Wolfe, T. L. An assessment of the impact of pollution on global cloud albedo. *Tellus* **1984**, *36B*, 356-366.

Twomey, S. Aerosols, clouds and radiation. *Atmos. Environ.* **1991**, *25A*, 2435–2442.

Uzel, S.; Chappell, M. A.; Payne, S. J. Modeling the Cycles of Growth and Detachment of Bubbles in Carbonated Beverages. *J. Phys. Chem. B* **2006**, *110*, 7579–7586.

Vehkamäki, H.; Kulmala, M.; Napari, I.; Lehtinen, K. E. J.; Timmreck, C.; Noppel, M.; Laaksonen, A. An improved parameterization for sulfuric acid-water nucleation rates for tropospheric and stratospheric conditions, *J. Geophys. Res.* **2002**, *107*, (D22), 4622.

Vohra, V.; Heist, R. H. The flow diffusion chamber: A quantitative tool for nucleation research. *J. Chem. Phys.* **1996**, *104*, 382−395.

Volmer, M.; Weber, A. Keimbildung in übersättigten Gebilden, *Z. Physik. Chem.* **1926**, *119*, 277–301.

Wagner, P. E.; Anisimov, M. P. Evaluation of nucleation rates from gas flow diffusion chamber experiments. *J. Aerosol Sci.* **1993**, *24*, S103−S104.

Wagner, P. E., Kaller, D., Vrtala, A., Lauri, A., Kulmala, M., and Laaksonen, A.: Nucleation probability in binary heterogeneous nucleation of water-*n*-propanol vapor mixtures on insoluble and soluble nanoparticles. *Phys. Rev. E* **2005**, *67*, 021605-[1-12].

Wedekind, J.; Hyvärinen, A.-P.; Brus, D.; Reguera, D. Unraveling the "pressure effect" in nucleation. *Phys. Rev. Lett.* **2008**, *101*, 125703.

Wilson, C. T. R. Condensation of Water Vapour in the Presence of Dust-Free Air and Other Gases. *Phil. Trans. Roy. Soc.* **1897**, *A 189*, 265-307.

Wilson, C. T. R. On the Comparative Efficiency as Condensation Nuclei of Positively and Negatively Charged Ions. *Phil. Trans. Roy. Soc.* **1900**, *A 193*, 289-308.

Wingenter, O. W.; Elliot, S. M.; Blake, D. R. New Directions: Enhancing the natural sulfur cycle to slow global warming. *Atmos. Environ.* **2007**, *41*, 7373-7375.

Young, L. H.; Benson, D. R.; Kameel, F. R.; Pierce, J. R.; Junninen, H.; Kulmala, M.; Lee, S.-H. Laboratory studies of H2SO4/H2O binary homogeneous nucleation from the SO2+OH reaction: evaluation of the experimental setup and preliminary results. *Atmos. Chem. Phys.* **2008**, *8*, 4997–5016.

Yue, G. K.; Hamill, P. The homogeneous nucleation rates of H_2SO_4-H_2O aerosol particles in air. *J. Aerosol Sci.* **1979**, *10*, 609-614.

Zeldovich, J. B. Theory of the formation of a new phase, Cavitation. *J. Exp. Theor. Phys.* **1942**, *12*, 525-538.